Quantifying marine growth on pipelines with archival remotely operated vehicle footage – a case study

Ben Bayley [1], Terry Griffiths [2], Fabrizio Pistani [2], Petra Helmholz [1], David Belton [1], and Iain Parnum [1]

[1] School of Earth and Planetary Sciences, Curtin University, Bentley Western Australia
GPO Box U1987, Perth, WA, Australia – {ben.bayley@graduate.curtin.edu.au; I. Parnum; D.Belton; Petra.helmholz}@curtin.edu.au

[2] Aurora Offshore Engineering, Unit 2, 186 Hampden Road, Nedlands, WA, Australia {terry; fabrizio}@aurora-oe.com

Keywords: Structure-from-motion, Marine Growth, Underwater Photogrammetry, ROV, Pipelines

Abstract

Marine growth can substantially affect the hydrodynamic properties of subsea infrastructure. The ability to accurately quantify this growth is essential for designing and maintaining subsea structures. Traditionally, quantifying marine growth has been done by applying simple ratio equations putting in relationship the known distance of an object and its length observed in the image to the length of an unknown object only observed in an image. This method is very sensitive if measurements are not taken in the same plane. Hence, this study aims to establish a method for creating a 3D model of a subsea pipeline segment based on Structure from Motion (SfM). The proof of concept is done using a case study. For this study, Remotely Operated Vehicle (ROV) footage from a 2019 inspection survey is utilised. The scenario in which the procedure is tested represents a difficult, but realistic test case. Despite the lack of metadata, video quality and obstructions (e.g. watermarks), meaningful results were produced. The SfM workflow included masking obstructions (e.g. watermarks), and an iterative camera alignment procedure to generate 3D models, enabling the measurement of marine growth using either the models or ortho images created. While the resulting models were sufficiently accurate to provide meaningful measurements for harder growth types, the method faced challenges in accurately modelling softer growth types, suggesting the need for further refinement. Nevertheless, SfM was proven to be a more reliable method of measuring biofouling than the ratio approach that been traditionally used.

1. Introduction

Marine growth, also known as biofouling, typically describes the process in which aquatic organisms settle and develop on artificial structures and is a serious issue for many maritime industries (Maduka et al., 2023). The development and inhabitation of marine organisms on underwater infrastructure gradually led to substantial implications for engineering, affecting both maintenance and design aspects. A greater understanding of marine biofouling is a priority for researchers, and with the continued growth of maritime industries, it has a global relevance (McLean et al., 2020).

Maintenance, inspection, and repair activities for subsea infrastructure, including wells, jackets, mattresses, and pipelines, are frequently conducted using remotely operated vehicles (ROVs). Previous studies have used structure-from-motion (SfM) to map and measure marine growth and subsea structures (Kikuzawa et al., 2018; Bayley and Mogg, 2020; Lange, 2020; Rofallski et al, 2020). However, the data capture for these studies has been carefully planned and undertaken in near-ideal situations. Part of the challenge of this study was to adapt the methods developed previously to a far more challenging scenario as we are dealing with legacy data.

Globally, these inspection campaigns generate millions of hours of footage, documenting the structures and their associated marine life. Leveraging this extensive footage to extract valuable data holds potential benefits for both, the industry and the scientific community (McLean et al., 2020). An issue with historical footage is that some metadata (such as position information) may no longer be available or was not collected as part of the original survey.

In this study, a survey designed to observe and document spanning is being adapted to model marine growth. In using archival footage, the scenario of not having ideal data would be common, and thus developing processes that can work in less-than-ideal situations, would be important in allowing the utilisation of vast stores of footage.

This study aims to prove the concept that photogrammetry can be used to harness archival ROV footage of a pipeline and to measure the growth of biofouling on the pipeline. As part of this study, three-dimensional models from the footage were created which consequently allowed for measurements of the marine growth present on the pipeline. The genesis of this study originated from an industry-driven need to quantify marine growth more accurately and to model its impacts on the hydrodynamics of the pipeline.

The paper is structured as follows. First, in (Section 2) the background section, we present the existing workflow to measure biofouling on pipelines, and will show how Structure-from-motion (SfM) can enhance the existing method. Next, in Section 3, the dataset used for this proof-of-concept study is introduced. Our method for the processing of the data is introduced in Section 4, and is followed by results (Section 5) and conclusions and discussions (Section 6).

2. Background

Video capture are, and will continue to be, key elements in inspection surveys, but subsea photogrammetry differs from in air, additional factors including suspended particles in the water, random refraction and the effects of artificial lighting must be considered (Chemisky et al., 2021). Traditional photogrammetric methods need to know either the position and orientation of the camera(s), the coordinates of control points to reconstruct a scene, or use a camera calibration frame (Luhmann et al, 2014; Shortis, 2019; Mufti et al., 2023). In

This contribution has been peer-reviewed. The double-blind peer-review was conducted on the basis of the full paper.
https://doi.org/10.5194/isprs-annals-X-4-2024-45-2024

comparison, the control and positioning of an ROV often being considerably more difficult than for a terrestrial camera platform.

Quantifying marine growth using archival footage has been done so far by applying simple ratio equations. Close to the biofouling being measured, the distance of a known object in the images is selected. The ratio of the pixel distance which covers the known object and the known distance of this object in [m], is then applied to the pixel distance of the unknown object (the biofouling). An example is shown in Figure 1. The diameter of the pipe is known, and its pixel distance is observed in the image (white line in Figure 1). Then, the distance of the biofouling (black line in Figure 1) is selected and its metric distance is derived.

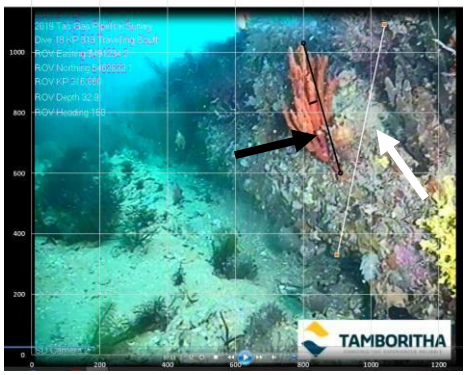

Figure 1. Old method of measuring using ratio of pixel distance.

However, this method is prone to errors if the two distances are not located in one plane. In this case, the displacement in the image (Δr) will depend on the off-plane distance (Δh) as well, the distance to the image centre (r), as well as the distance of the camera to the object (h) as shown in equation 1 (Luhman et al., 2014).

$$\Delta r = r / h \cdot \Delta h \quad (1)$$

The displacement Δr should be considered when the ratio equation is applied. However, this is usually not done.

The existing methods can be enhanced by 3D models derived by Structure-from-motion (SfM). SfM operates on a principle similar to stereoscopic photogrammetry, allowing for the creation of 3D models from overlapping images. The key distinction between traditional methods and SfM lies in the absence of control points in the latter. Camera positions and orientations are determined as part of an iterative bundle adjustment process based on features derived from the overlapping images. SfM is most effective when the entirety of the 3D scene can be captured from a wide array of positions or using a moving camera (Westoby et al., 2012).

In SfM, extracted features are tracked between images, and these features are subsequently used to estimate the camera's position. This process is iteratively executed to refine the positions. Due to the absence of control points in SfM, the results lack scale and orientation, resulting in point clouds being created in object space. Key points are identified in each image, and the quantity detected heavily depends on image texture and resolution. The photograph's density, sharpness, and resolution will dictate the quality of the resultant point cloud. The minimum requirement for effective operation is for corresponding features to be visible in a minimum of three photographs (Westoby et al., 2012).

3. Dataset

The videos used for this research were captured during an inspection survey conducted in 2019 of the TasGas pipeline, which was installed in 2002, between northern Tasmania and Victoria, Australia. Video footage was obtained from three cameras mounted on the ROV capturing the right, left, and top of the pipeline. The cameras positioned on the left and right sides of the pipeline were standard definition (SD), while the camera situated above the centre of the pipeline captured footage in high definition (HD). Unfortunately, no information regarding the specifications of the cameras, their positions relative to each other, or their relationship to the ROV was provided. The only additional information available was positional data embedded in the video in the form of text, which contained easting, northing, kilometre point (KP), depth, and heading.

4. Methods

The SfM processing procedure is summarised in Figure 2, with the individual steps detailed in the sections below. For image processing, the Metashape software was utilised due to this project being an industry-led project.

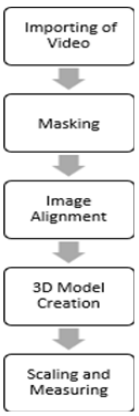

Figure 2. Structure-from-motion processing workflow.

4.1 Importing of video

The initial step in the workflow, involves importing the video into the Metashape software. Within this stage, the specific portion of the video is to be imported and the frame jump parameter can be chosen. The video was captured at a rate of 20 frames per second for all three cameras, and to ensure adequate overlap between images, a frame jump of 5 was employed during the import process. Metashape subsequently converts and saves the video as individual images, from which the subsequent stages of the process are carried out. Should additional images be required, an additional segment of the video could be imported, and the resultant images incorporated into the existing dataset.

4.2 Masking

In this study, the ROV video footage frequently contained text, watermarks, or pieces of equipment within the image (Figure 3). These elements can pose challenges when attempting to construct a 3D model. The masking process was conducted in Metashape. The areas to be masked were manually outlined on

This contribution has been peer-reviewed. The double-blind peer-review was conducted on the basis of the full paper.
https://doi.org/10.5194/isprs-annals-X-4-2024-45-2024 | © Author(s) 2024. CC BY 4.0 License.

the image (Figure 3). The masking was performed manually as this research is a proof-of-concept paper only. This step can easily be automated.

Two separate masks were created: one for the centre camera and another for the left and right cameras, as they exhibited different obstructions. Each mask was then saved to a file for easy access and application to images. The application of the masks occurs after the images are loaded into the project. The mask is imported and set to 'apply to all images', ensuring that every image in the set receives the mask.

Figure 3. Example image used, and the masking is shown as shaded areas.

4.3 Image Alignment

The most critical phase of the procedure is the alignment of the images, which entailed estimating the camera parameters and their positions using a bundle adjustment. The absence of camera parameter information, coupled with a suboptimal geometry for their estimation, and variable image clarity, rendered image alignment particularly challenging. Efforts to align entire image sets frequently resulted in the 'spiralling' of camera positions (Figure 4), or sometimes only partial sections are being aligned successfully. Despite multiple attempts with different frame jumps and pipeline sections, the images could not be reliably aligned using large single sets of images. Effort was also made to utilise the embedded positional data; the data was manually written into a text format for a small section of pipe for a single camera and imported into Metashape. The alignment conducted using the reference data showed no measurable difference from those completed without it, so it was not used in further processing given the considerable time required to create the text file.

Through experimentation, an incremental image alignment approach was utilised to achieve a more reliable alignment process that could accurately determine camera positions and parameters (Figure 5). This method commenced with the initial alignment of a small subset of photos, ranging from 10 to 20. Subsequently, additional photos were incrementally added, with 10 photos being added in this study (as the total number of images in the set increased, a larger number of images could be added at each step). The masks were applied to the newly added images, and the entire photo set was aligned without resetting the initial alignment results. A gradual selection process, similar to that employed by Lange and Perry (2020), was implemented to eliminate tie points with high reprojection error. Given that the total number of points in the point cloud was lower than in previous studies to use this approach, the selection process was more conservative with only 10-15% of points being selected and removed. Following the removal of these points, the camera calibration was optimized again, before adding in another set of images. This procedure was iterated until the entire area of interest was covered.

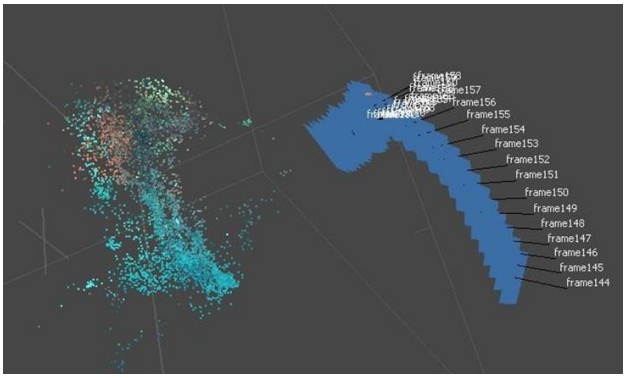

Figure 4. An example of an incorrect alignment of pipeline data.

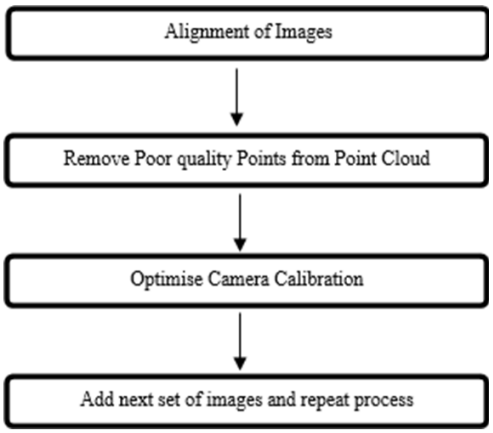

Figure 5. Iterative alignment process.

Figure 6 illustrates the resulting camera positions from the alignment of the left camera, which more closely mirrors the path of the ROV, signifying a successful resolution of the bundle adjustment. This process was carried out for each of the three cameras along the area of interest. At this point a camera report can be generated inside the software to check the quality of the alignment.

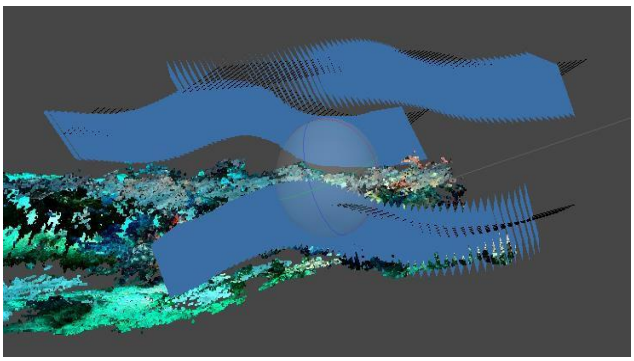

Figure 6. Successful image alignment of pipeline data. Clearly showing the three cameras (one centre and two to each site) installed on the ROV.

4.4 3D Model Creation

The image alignment process creates a sparse cloud of tie points, from these tie points several 3D models can be

computed. The first model made was a dense point cloud (Figure 7). This model is likely the most useful in 3D analysis of the pipeline and the growth, as individual points can be picked to quantify the growth. The next model that was created was a textured mesh (Figure 8), which overlays the images onto a mesh created from the dense point cloud. While the textured mesh is useful for visual analysis of the pipe, the interpolation used to create the mesh lessens the level of detail available compared to the dense point cloud, due to the complexity of the data. Perhaps the most useful output for this study, was the creation of orthoimages, as these allowed for the 3D measurement of the growth.

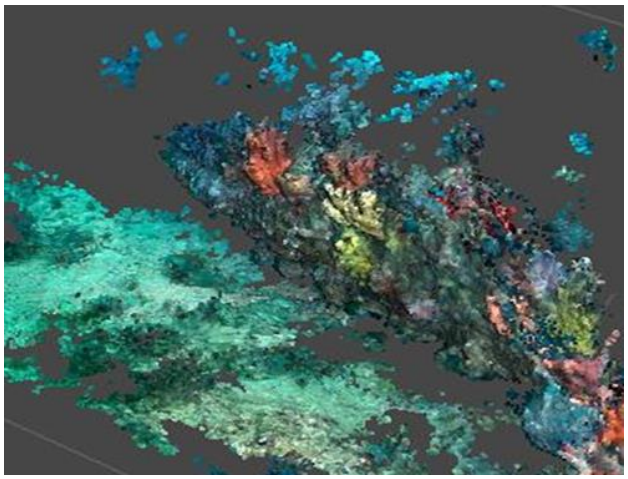

Figure 7. Dense point cloud of the pipeline.

Each of the cameras was processed separately up to the creation of the dense point cloud, at this point, to make a full model using all three cameras, the chunks that each camera was processed in must first be aligned and then merged (Figure 9). The alignment can be completed using a combination of either the tie points, dense point cloud, mesh, or markers. Markers in Metashape act as a control point within the object space, markers can be manually picked at common points between the images for one camera or between cameras.

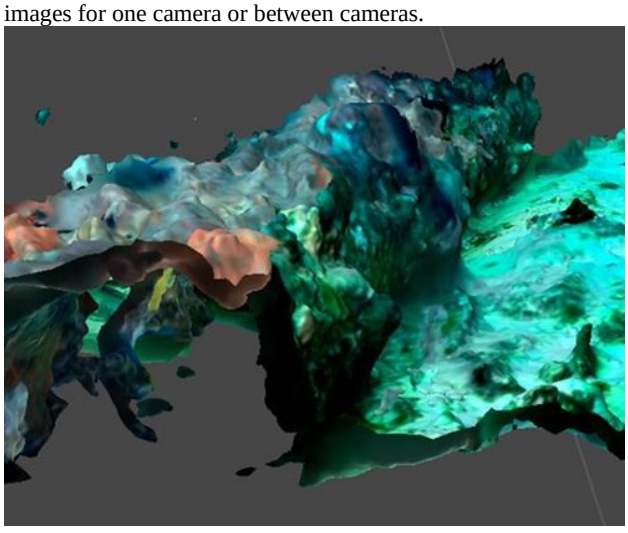

Figure 8. Textured mesh of the pipeline.

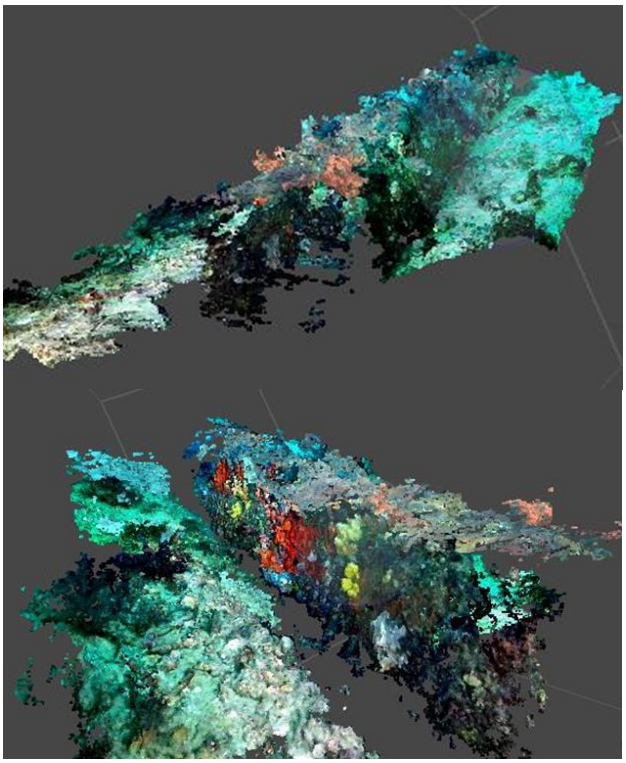

Figure 9. Combined model: Top: Right side of the pipe. Bottom: Left side of the pipe.

4.5 Scaling and measurements

Given there were no control points or scale bars present on or around the pipeline, the 3D models created have no metric scale, nor are orientated to the real environment in which they were captured. As orientation was not important for this study, the focus was on scaling. The scaling was completed using a scale factor that scales the entire model by the same factor. For this project, the scaling can be completed because of the known diameter of the pipe of 432mm. Further distances can be calculated between two cameras from the positional data displayed in the images. The model was scaled until these distances matched the reference distances (Figure 10). The scaling in Metashape was limited to only the whole model scaling using a scale factor (see Figure 10).

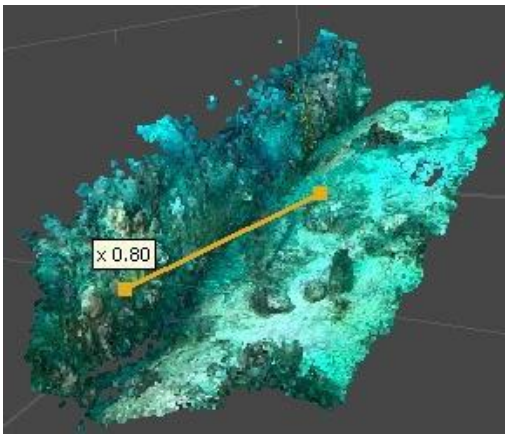

Figure 10. Scaling using Metashape.

For this study, measurements were made of the same sponges and algae in all three models. The measuring of the marine

growth could be done either on the dense point cloud, textured mesh or orthoimages. Measuring in Metashape is done by picking two or more points on the model and is a simple process. Attention was paid to where the previous studies had measured from as this is an obvious source of error in the measurements, the picking of these points was far easier on the photos given they had not been distorted at all to fit the 3D models and showed the greatest level of detail. Measurements taken using the dense point cloud returned almost identical results, although picking the points to measure from was more difficult, as the level of detail was not as great as in the photos. Any difference between the two measurements is likely due to human error in picking the two points to measure between.

5. Results

The main challenge for the evaluation is missing reference data as we deal with legacy data. Instead, we have performed first a qualitative analysis (visual assessment) followed by the comparison of measurements derived from the traditional method with the new proposed method.

5.1 Qualitative Assessment

Looking at the models created, it was clear that the scene had been correctly reconstructed, as there are no major errors with the point cloud. It did, however, show some weaknesses in the models. In all models created, a slight bending of the pipe was present. Overall, the bend was gradual, the greatest extent of it is present at either end of the area modelled. The bending is a known issue, and is caused due to a weak estimation of the camera calibration parameters due to the lack of control or being able to change the configuration in which the images have been taken (Griffiths, D. and Burningham, 2019). While this bend will impact any measurements performed along the pipeline, it should not, or only very little, impact the measurements perpendicular to the image path. Hence, it is likely not to have a significant effect on the marine growth being assessed.

The visual inspection of the models also shows “empty” areas behind marine growth. This is a result of the camera angle and the path of the ROV. Essentially only one face of the sponges could be observed, meaning accurate volumetric analysis is prohibitive.

Another visually apparent result, was the effect of the soft algae growth. Firstly, tie points were not able to be extracted from image areas showing soft alga. This was caused by the algae moving between image frames and missing distinct features. In contrast, areas of seabed or hard growth had far more tie points found.

Lastly, looking at the combined model of the entire pipe the bending previously mentioned has resulted in some, small offsets between the three cameras. This was again most prominent at the ends of the area modelled. The alignment between the left and centre cameras was more difficult to achieve given the left side of the images from the centre camera was masked due to the embedded text and the ROV frame, thus the available number of tie points was far fewer.

5.2 Quantitative Assessment

The quantitative analysis compares measurements taken using the traditional method and measurements derived from the 3D reconstruction. As introduced in the background section, the traditional method is done simply by scaling the pipe and marine growth from the 2D image using basic ratio equations (Figure 1).

The measurements in Metashape are taken using the results from the creation of 3D models. Given the quality of the models, it was found to be easier to take measurements on the images themselves in which the marine growth is present. These images are orthoimages and distances are assumed to be in object space. An example is presented in Figure 11 which shows a digitate sponge (Sponge 1).

Figure 11. Derived measurement of a digitate sponge using an ortho-image.

Two sponges one algae were measured using the traditional and the SfM method shown here for comparison (Table 1). The difference between the two methods was small for the sponges (maximum of 2.5 cm). Whereas, the measurements of the algae, showed a much larger difference between the two methods. The traditional method gave a distance of 18.6 cm, and the SfM method a distance of 27.5 cm. The suspected reason behind the difference is the issue related to the algae’s movement in the currents. Consequently, the point cloud around the algae is far sparser and more inconsistent. However, the movement of the algae could also impact the measurement using the traditional method, due to the movement in and out of the optical plane to perform the measurements. Analysis of the video would suggest the algae was no longer than the digitate sponge (sponge 1). Thus, an error is more likely to be present in the measuring of the algae using the SfM based method.

	Traditional Method (cm)	Method based on SfM (cm)	Difference (cm)
Sponge 1	24.8	22.3	2.5
Sponge 2	24.9	27.1	2.2
Algae	18.6	27.5	8.9

Table 1. Biological growth measurements.

Another way to assess the quality of the model is to look at the accuracy of the point cloud itself, Metashape can generate a processing report that includes such data. The ground resolution of the point cloud was 1.5 mm/pixel and the reprojection error was 0.481 pixels, these values indicate the point cloud closely matched the real scene.

6. Conclusion

The scenario in which the SfM procedure for measuring marine growth was tested, represents a difficult, but realistic test case. Given the lack of metadata, video quality and obstructions (e.g. watermarks), having been able to produce meaningful results

here shows its promise in future works. The results indicate that the procedure developed using SfM can provide suitable measurements of marine growth on subsea structures. This is true, especially for hard growth. Softer growth is more difficult to model due to matching challenges. Nevertheless, the use of SfM for measurement of biofouling is a more accurate approach than the traditional approach of applying simple ratio equations, especially if the scaling object and the biofouling to be measured are not in the same plane. Moreover, the error of the ratio method increases, as the separation in planes of the scaling object and the measurement target increases.

The scope for future work in this area is large, specifically relating to this study. Further works that have access to camera details or positions could provide better results, different water conditions and camera orientations would also provide interesting studies. Additionally, evaluation of open-source photogrammetry software solutions (Vacca, 2020), would make this workflow more accessible. In a broader sense, the ability to create 3D models from legacy data could help the creation of digital twins, for CFD modelling, monitoring of changes to biofouling could also be aided by such development (Chen et al., 2022).

Acknowledgements

The authors would like to thank the team at Aurora Offshore Engineering, and Wacek Lipski and Palisade Integrated Management Services for their support and assistance on this project. Data processing was carried out using the 3D PC part of the 3D Imaging Hub at Curtin University.

References

Bayley, D. T., & Mogg, A. O. 2020. A protocol for the large-scale analysis of reefs using Structure from Motion photogrammetry. Methods in Ecology and Evolution, 11(11), 1410-1420.

Chemisky, B., Menna, F., Nocerino, E., & Drap, P. 2021. Underwater survey for oil and gas industry: A review of close range optical methods. *Remote Sensing* (Basel, Switzerland), 13(14), 2789. doi.org/10.3390/rs13142789

Chen, B.-Q., Videiro, P. M., & Guedes Soares, C. 2022. Opportunities and Challenges to Develop Digital Twins for Subsea Pipelines. *Journal of Marine Science and Engineering*, 10(6), 739. doi.org/10.3390/jmse10060739

Griffiths, D., & Burningham, H. 2019. Comparison of pre-and self-calibrated camera calibration models for UAS-derived nadir imagery for a SfM application. Progress in physical geography: earth and environment, 43(2), 215-235.

Kikuzawa, Y. P., Toh, T. C., Ng, C. S. L., Sam, S. Q., Taira, D., Afiq-Rosli, L., & Chou, L. M., 2018. Quantifying growth in maricultured corals using photogrammetry. *Aquaculture Research*, 49(6), 2249-2255. doi.org/10.1111/are.13683

Lange, I. D. & Perry, C. T., 2020. A quick, easy and non-invasive method to quantify coral growth rates using photogrammetry and 3D model comparisons. *Methods in Ecology and Evolution*, 11(6), 714-726. doi.org/10.1111/2041-210X.13388

Luhmann, T., Robson, S., Kyle, S., & Boehm, J., 2014. Close-range photogrammetry and 3D imaging. Berlin, Germany & Boston, MA: De Gruyter. doi.org/10.1515/9783110302783

Maduka, M., Schoefs, F., Thiagarajan, K., & Bates, A. 2023. Hydrodynamic effects of biofouling-induced surface roughness – Review and research gaps for shallow water offshore wind energy structures. *Ocean Engineering*, 272, 113798. doi.org/10.1016/j.oceaneng.2023.113798.

McLean, D. L., Parsons, M. J. G., Gates, A. R., Benfield, M. C., Bond, T., Booth, D. J., Bunce, M., Fowler, A. M., Harvey, E. S., Macreadie, P. I., Pattiaratchi, C. B., Rouse, S., Partridge, J. C., Thomson, P. G., Todd, V. L. G., & Jones, D. O. B. 2020. Enhancing the Scientific Value of Industry Remotely Operated Vehicles (ROVs) in Our Oceans. Frontiers in Marine Science, 7. doi.org/10.3389/fmars.2020.00220.

Mufti, A., Helmholz, P., Parnum, I., & Belton, D. 2023. Introduction and Validation of a Novel Calibration Frame. The International Archives of the Photogrammetry, Remote Sensing and Spatial Information Sciences, 48, 1935-1942.

Rofallski, R., Tholen, C., Helmholz, P., Parnum, I., & Luhmann, T. 2020. Measuring artificial reefs using a multi-camera system for unmanned underwater vehicles. International Archives of the Photogrammetry, Remote Sensing and Spatial Information Sciences, 43(B2), 999-1008.

Shortis, M,. 2019. Camera calibration techniques for accurate measurement underwater. 3D recording and interpretation for maritime archaeology, 11-27.

Vacca, G. 2020. WEB open drone map (WebODM) a software open source to photogrammetry process. In Fig Working Week 2020. Smart surveyors for land and water management.

Westoby, M. J., Brasington, J., Glasser, N. F., Hambrey, M. J., & Reynolds, J. M. 2012. ‘Structure-from-Motion’ photogrammetry: A low-cost, effective tool for geoscience applications. *Geomorphology* (Amsterdam, Netherlands), 179, 300-314. doi.org/10.1016/j.geomorph.2012.08.021